FURTHER STUDIES ON THE TRANSIENT STABILITY OF SYNCHRONOUS-SYNCHRONOUS ROTARY FREQUENCY CONVERTER FED RAILWAYS WITH LOW-FREQUENCY AC HIGH-VOLTAGE TRANSMISSION

LARS ABRAHAMSSON, JOHN LAURY & MATH BOLLEN

Electric Power Engineering, Luleå University of Technology, Skellefteå, Sweden.

ABSTRACT

This paper continues the pursuit of getting a deeper understanding regarding the transient stability of low-frequency AC railway power systems operated at 16 ⅔ Hz that are synchronously connected to the public grid. Here, the focus is set on such grids with a low-frequency AC high-voltage transmission line subject to a fault. The study here is limited to railways being fed by different distributions of Rotary Frequency Converter (RFC) types. Both auto transformer (AT) and booster transformer (BT) catenaries are considered. No mixed model configurations in the converter stations (CSs) are considered in this study. Therefore, only interactions between RFCs in different CSs and between RFCs, the fault, and the load can take place in this study. The RFC dynamic models are essentially two Anderson-Fouad models of synchronous machines coupled mechanically by their rotors being connected to the same mechanical shaft. Besides the new cases studied, also a new voltage-dependent active power load model is presented and used in this study.

Keywords: 16 ⅔ Hz, electromechanical dynamics, frequency converters, power systems, railway, synchronous machines, train load modelling, transient stability.

1 INTRODUCTION

In previous studies [1, 2], the impact of mixed converter station (CS) populations of rotary frequency converters (RFCs) of different types in terms of the transient stability was investigated. Those studies, as well as this study used models describing 16 ⅔ Hz AC railways operated synchronously to the feeding public three-phase 50 Hz grid, such as the ones in Scandinavia. In this paper, the CSs only contain one converter unit per CS, as described in section 3.3.

Transient stability of low-frequency AC synchronous railways involving the railway high-voltage transmission (HVT) line has been studied in [1], which this paper is an extension of in terms of more study cases, a different fault (type and) location studied, and a new load model. This paper also considers both booster transformer (BT) and autotransformer (AT) catenaries, whereas [1] only considers BT catenaries. Consideration and comparison between BT and AT catenaries have been made in [2], but that study focuses on railway grids not strengthened by an HVT system.

Besides that, in [3], the transient stability of HVT equipped railways was studied for the first and only time before [1]. In that study however, the classical model of synchronous machines were used for the RFC modeling. In [1, 2], the Anderson-Fouad model is used, the complete theoretical framework of the used RFC model is presented in [4]. The study [3] gives an insight on how a converter station behaves during a severe disturbance. However, the study does not show how converter stations interact with each other.

Generally, studies done and published about stability of low-frequency AC railways are few, especially for transient stability of synchronously operated railway grids. For a deeper literature review, the reader is recommended to refer to the references of the work referenced to in this paper.

ISSN: 2056-3272 (paper format), ISSN: 2056-3280 (online), http://www.witpress.com/journals
DOI: 10.2495/EQ-V3-N4-266-276

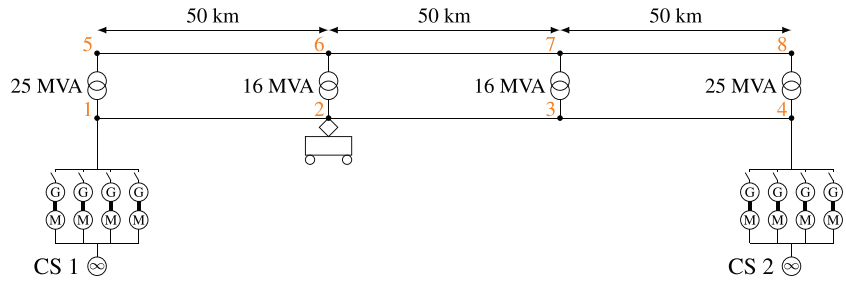

Figure 1: Illustration of the system studied. Node numbers in orange.

The paper is organized as follows: this introduction of section 1 is followed by section 2 where the models used are either described in detail or references are made to publications where they are. The models that are completely new in this paper are thus the core focus of section 2. After that, in section 3 a description of the cases studied and the overall simulation study setup can be found. The major part of the paper is section 4 which is dedicated into graphically presenting and in text describing and interpreting the results. Finally, in section 5 the results of the paper are discussed and some conclusions are drawn.

By obvious reasons, the models and parameters used in this paper are adjusted for the Scandinavian (and former East German) $16\frac{2}{3}$ Hz synchronous railways, but they could easily be adapted for the North American 25 Hz counterpart.

2 MODEL DESCRIPTIONS

For the admittance matrix creation, the principle of [5, Figure 2.4], in particular for the AT catenary modeling, has been followed.

2.1 Steady state

The steady state pre-fault load flow solution is using RFC and grid models well-described in [5–7], and their linkage to the dynamic models during fault and post fault are described in depth in [4].

In the pre-fault load flow, the train load P_D is set to 10 MW. The static load-flow is done in GAMS similar to the ones made in [5, 8], but for only one time step and with fixed train loads.

2.2 Dynamic rotary frequency converter (RFC) and grid models

As indicated in section 1, the dynamic RFC models used in this paper are the same ones as the ones presented in detail in [4], and the same ones as used in [1, 2]. The same goes for the grid model and the RFC-load-grid interconnections during the electromechanical simulations.

The dynamic models are implemented in Simulink as in [1, 2, 4].

2.3 Load model for the dynamic part of the study

In real life, the transient load behaviour in railways is of a complicated nature. Somewhat more detailed load models are presented in for example [9]. Those models are however

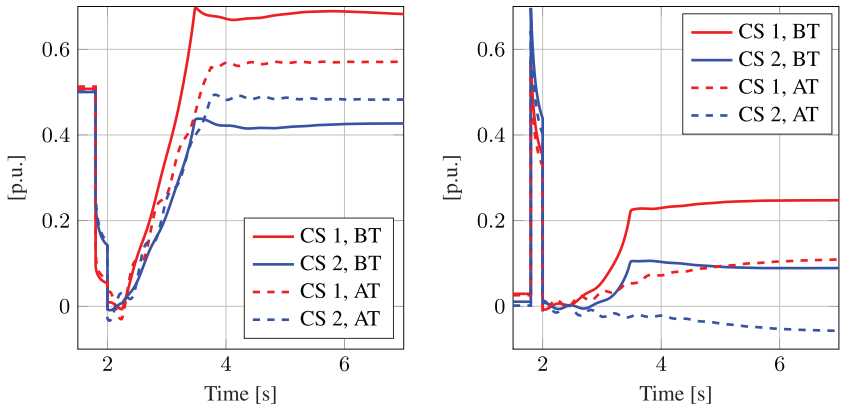

(a) Active power (b) Reactive power

Figure 2: The active power outputs of the converter(station)s in the system. Case 1, voltage regulated active power load.

linearized and used for small signal/disturbance analysis, so for example current limitation will not be of consider there. The model proposed in this paper have in different ways, simplistic as it is, in-built current limitations.

A totally constant-power load is neither useful, nor realistic. During a fault, the voltage level at the load can sink significantly, and a truly constant load would in such a situation imply currents tending to infinity. The model proposed and used here is inspired by [3] where it is stated that locomotives exposed to voltages below 10 kV zeroes the consumed active power. The consumed power remains zero until the voltage has returned to a *relatively high level* and waits after that for another 200 ms. Thereafter, power is ramped up to its previous value for 1.5 seconds. Also here, as in [3], the exact behaviour of locomotives is admitted to be much more complicated in real-life. This is however, one step forward in the model development procedure.

The model can best be described in algorithmic form for each time step t, with $P_{D,\text{init}}$ being the pre-fault active power consumption reference, $P_{D,\text{ref},}$ for the train, and with the parameter l_1 initiated to be valued 0:

1. If $U_{\text{train}} < U_{\text{min 1}}$. This is when the voltage goes below 10 kV.
   (a) Set $P_{D,\text{ref}}$ to 0.
   (b) Set the parameter l_1 to 1.
   (c) Set the parameter t_{stamp} to t
2. If instead $(U_{\text{train}} \geq U_{\text{min 2}} \wedge l_1 = 1) \vee (l_1 = 2 \wedge (t - t_{\text{stamp}}) \leq 0.2)$. This is when the voltage has earlier been below 10 kV and has thereafter risen to above 14.25 kV for the first time, or has done so less than 0.2 seconds ago.
   (a) Set $P_{D,\text{ref}}$ to 0.
   (b) Set l_1 to 2.
3. If instead $((t - t_{\text{stamp}}) > 0.2) \wedge l_1 = 2$. This is when 0.2 seconds have passed after the train voltage has reached over 14.25 kV and not (yet) fallen below 10 kV again.
   (a) Set $P_{D,\text{ref}}$ to $P_{D,\text{init}} \cdot \dfrac{t - t_{\text{stamp}} - 0.2}{1.5}$

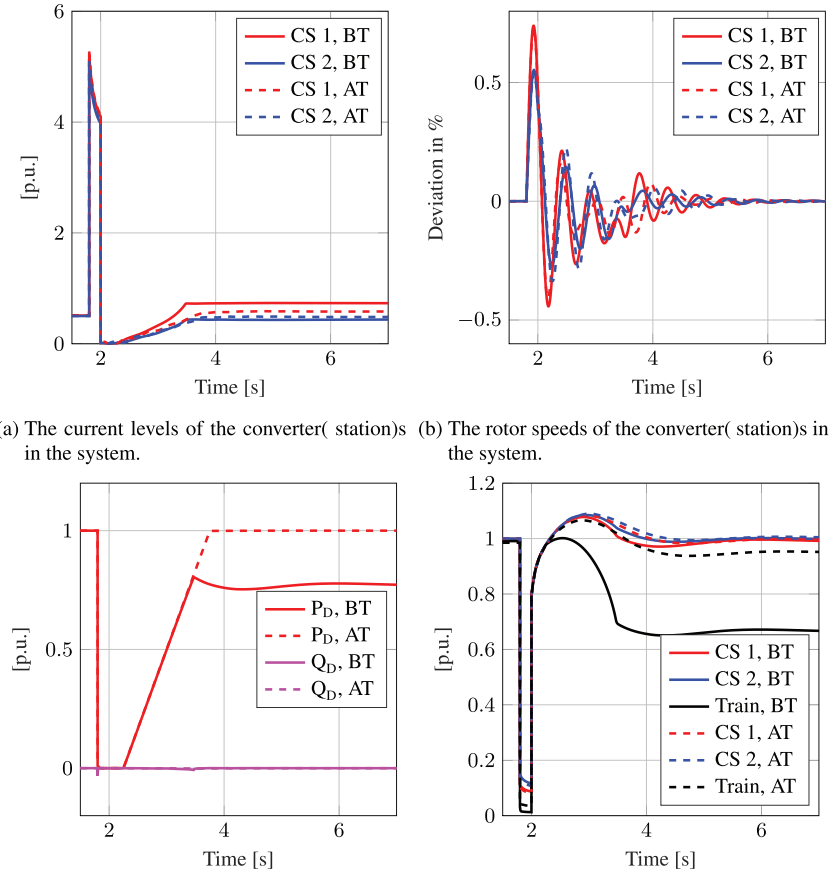

(a) The current levels of the converter(station)s in the system.

(b) The rotor speeds of the converter(station)s in the system.

(c) The active and reactive power consumptions of the trains in the system.

(d) The voltage levels of the trains and the converter stations in the system.

Figure 3: Case 1, voltage regulated active power load.

(b) If $P_{D,\text{ref}} \geq P_{D,\text{init}}$. This is as soon as the train power demand reference has returned to its initial value.
   i. Set $P_{D,\text{ref}}$ to exactly $P_{D,\text{init}}$.
   ii. Set l_1 to zero again.

4. If instead l_1 equals 1. This implicitly means that the voltage to have not risen up to 14.25 kV yet.

   (a) Just keep $P_{D,\text{ref}}$ at 0.
   (b) Update the value of t_{stamp} to t. The parameter t_{stamp} is updated like this until the voltage exceeds 14.25 kV.

5. Else
   (a) Set $P_{D,\text{ref}}$ to exactly $P_{D,\text{init}}$.

In the above, $U_{\text{min }1}$ is 10 kV and $U_{\text{min }2}$ equals 14.25 kV. The prior value is taken from [3], the latter from [10] according to which is the highest voltage level for which train tractive forces should not be limited.

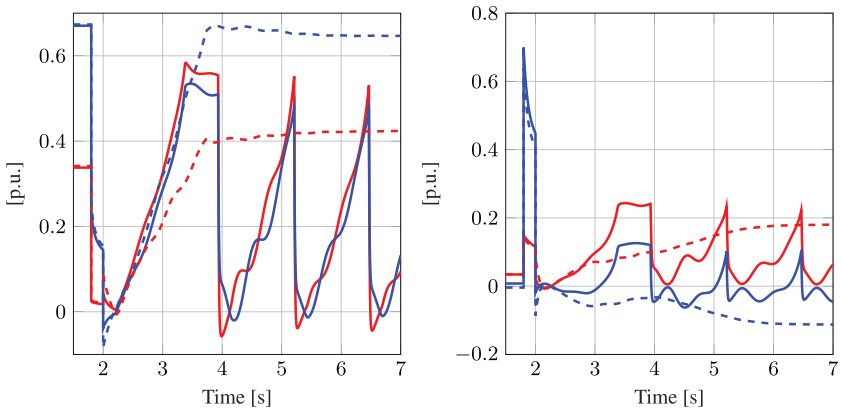

(a) Active power (b) Reactive power

Figure 4: Outputs of the converter(station)s in the system. Case 2, voltage regulated active power load. Legend valid for this figure can be found in Fig. 5(d).

For completion, $Q_{D,\mathrm{ref}}$ is set to zero all through the simulation, which implicitly can be seen in eqn (1).

In each time step t_s representing time $t = t\,(t_s)$, the power references $P_{D,\mathrm{ref}}$ computed are used together with the voltages to determine the load current of the train for the coming time step t_{s+1},

$$I_{D,\mathrm{ref}}^{\mathrm{unlim}}\left[t_{s+1}\right] = \frac{P_{D,\mathrm{ref}}\left[t_s\right]}{U[t_s]\angle -\theta[t_s]} \tag{1}$$

$$I_{D,\mathrm{ref}}^{\mathrm{lim}}\left[t_{s+1}\right] = \begin{cases} I_{D,\mathrm{ref}}^{\mathrm{unlim}}\left[t_{s+1}\right] & ,\left|I_{D,\mathrm{ref}}^{\mathrm{unlim}}\left[t_{s+1}\right]\right| \le I_{D,\max} \\ I_{D,\mathrm{ref}}^{\mathrm{unlim}}\left[t_{s+1}\right] \cdot \dfrac{I_{D,\max}}{\left|I_{D,\mathrm{ref}}^{\mathrm{unlim}}\left[t_{s+1}\right]\right|} & ,\left|I_{D,\mathrm{ref}}^{\mathrm{unlim}}\left[t_{s+1}\right]\right| > I_{D,\max} \end{cases} \tag{2}$$

but with the exception that a current limitation, where the modulus of the train load current cannot exceed $\mathrm{I}_{D,\max} \in \mathbb{R}$ is considered as well. In Figs. 3(c) and (d), one can for the BT catenary case see that without the eqn (2) current limitation, the load would have caused the voltage to go below 10 kV (≈ 0.61 p.u.). That happens repeatedly in, for example Figs. 5(c) and 5(d), where load current is smaller than $\mathrm{I}_{D,\max}$, but large enough to sink the voltage so deep that the train voltage protection system assumes that it is a fault occurring in the system.

3 DESCRIPTION OF THE CASE STUDY

3.1 General problem setup

General for the cases studied is the grid illustrated in Fig. 1, where the switches indicate that different RFC feedings are investigated in the four different cases. The connection and disconnection of RFCs typically take place on the railway side if not decomitted for a longer period [11, 12].

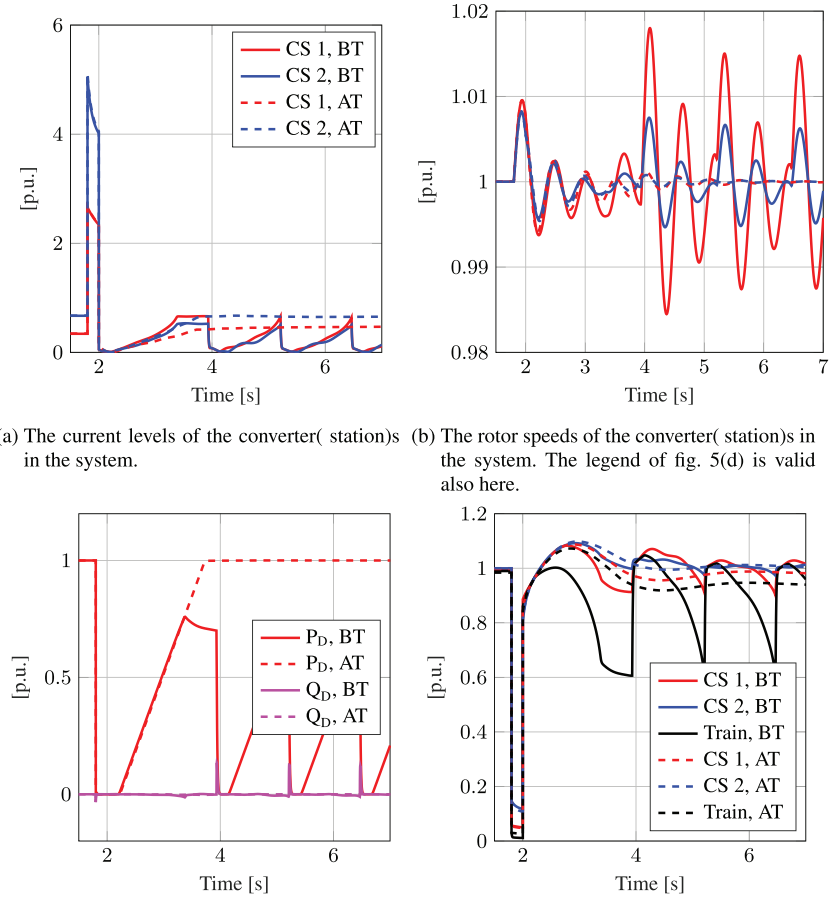

(a) The current levels of the converter(station)s in the system.

(b) The rotor speeds of the converter(station)s in the system. The legend of fig. 5(d) is valid also here.

(c) The active and reactive power consumptions of the trains in the system.

(d) The voltage levels of the trains and the converter stations in the system.

Figure 5: Case 2, voltage regulated active power load.

In each of the cases studied, a solid two-phase fault occurs right in the middle between nodes 5 and 6 in Fig. 1 at 1.8 seconds of time. After another 0.2 seconds, the entire connection to the HVT-system is disconnected as a measure of clearing the fault for the moment being.

3.2 Numerical parameters

As indicated in Fig. 1, the feeding section is 150 km, which is representative for the distances used in Sweden where the HVT grid is present. Moreover, between the CSs' 25 MVA transformer stations (TSs), there are two 16 MVA TSs connecting the catenary system to the HVT line. All TSs are distanced 50 km from each other. Two TSs between the TSs of the CSs occurs in Sweden, but three and four intermediate TS connections are more common [13].

For the load model of section 2.3, the current limit, $I_{D,\max}$, is defined as the current drawn by the vehicle at 10 MVA and at 14.25 kV – the lowest catenary voltage without limited tractive force according to [10].

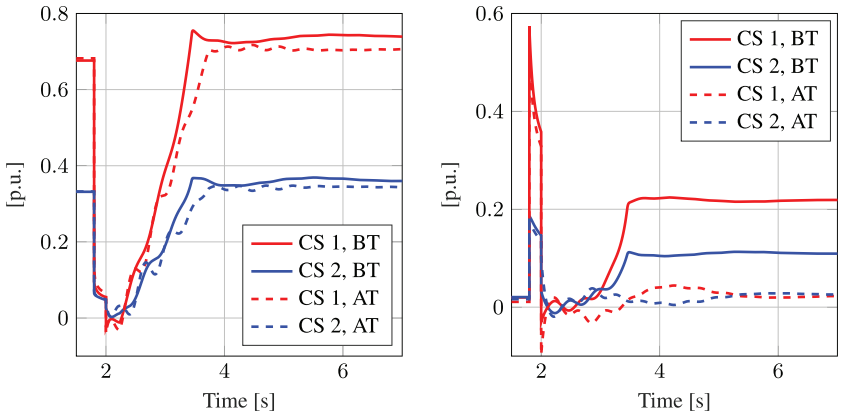

(a) Active power (b) Reactive power

Figure 6: The outputs of the converter(station)s in the system. Case 3, voltage regulated active power load.

The voltage droop (sometimes called compounding) of the RFCs at the railway side is set to 3%. In practical terms, it means that the terminal voltage at no-load should be 16.5 kV, and for generation of 10 MVAr reactive power, Q_G, the terminal voltage should be 16 kV.

The base power, S_b in the studies is set to 10 MVA, and the base voltage, U_b, on the catenary side is set to 16.5 kV. Line data of AT and BT catenaries are the same as used and presented in [1, 2, 4]. The step-up transformer data between catenary system and HVT system, as well as the HVT impedances, are the same as used in [1].

Parameters for the two (in Sweden most common) RFC types Q48/Q49 and Q38/Q39 are presented in detail in [4] and [9], respectively.

3.3 Case descriptions

Each of the four study cases consider AT as well as BT catenaries. Therefore, eight different cases are studied in this paper.

The RFC models used for feeding the railway varies between the four study cases. In:

Case 1 CS 1 as well as CS 2 of Fig. 1 have one RFC of type Q48/Q49 each committed in the study.
Case 2 CS 1 has one RFC of type Q38/Q39 committed, whereas CS 2 has one RFC of type Q48/Q49 committed in the study.
Case 3 CS 1 has one RFC of type Q48/Q49 committed, whereas CS 2 has one RFC of type Q38/Q39 committed in the study.
Case 4 CS 1 as well as CS 2 have one RFC of type Q38/Q39 each committed in the study.

4 RESULTS

4.1 Case 1

In Fig. 2(a) one can see that the load sharing is better for the AT catenary case. One can see that Fig. 2(b) shows disabilities of load sharing for both AT and BT. That might be explained

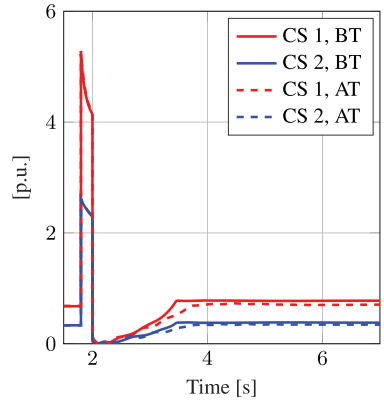

(a) The current levels of the converter(station)s in the system.

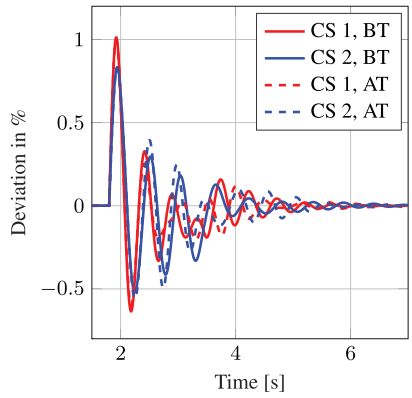

(b) The rotor speeds of the converter(station)s in the system.

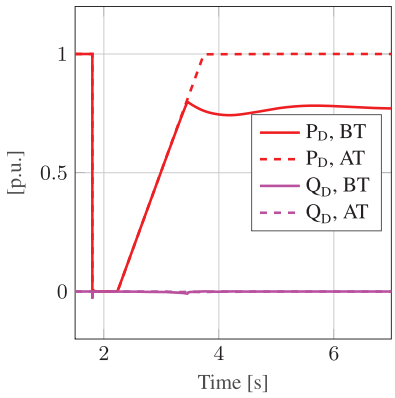

(c) The active and reactive power consumptions of the trains in the system.

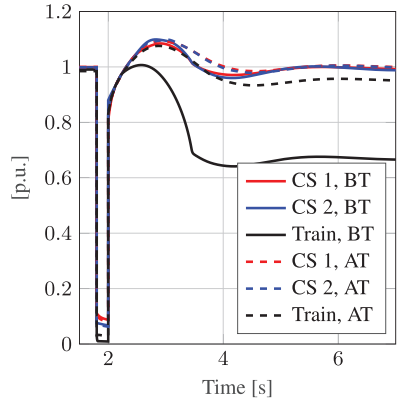

(d) The voltage levels of the trains and the converter stations in the system.

Figure 7: Case 3, voltage regulated active power load.

by the fact that this train model keep Q_D close to zero as shown in Fig. 3(c) for AT as well as BT feeding. Summing the reactive power output of the two CSs makes it closer to zero for the AT case – likely because of the AT system's lower impedances.

The currents of each CS is depicted in Fig. 3(a). The rotor oscillations get a smaller, second, disturbance in Fig. 3(b) in the same moment in time as the train load increase halts in Fig. 3(c) because of either load recovery for the AT system or current limitation for the BT system. System voltages are depicted in Fig. 3(d).

4.2 Case 2

The active powers of Fig. 4(a) reflect very well the active power loads of Fig. 5(c). The reactive power loads of Fig. 4(b) reflect the fault currents and the voltage fluctuations in Fig. 5(d) and reactive power losses caused by the loads in Fig. 5(c).

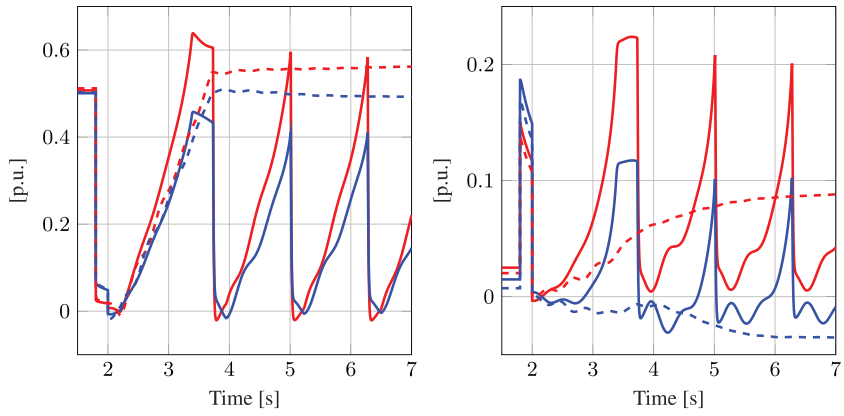

(a) Active power (b) Reactive power

Figure 8: The outputs of the converter (station)s in the system. Case 4, voltage regulated active power load. Legends useful for this figure can be found in Fig. 9(d).

The currents of the CSs are depicted in Fig. 5(a). The rotor oscillations in Fig. 5(b) are more affected by the train load regulation transients than by the fault, and the smaller RFC in CS 1 oscillates more in rotor speed deviations than the CS 2 RFC. Train loads in Fig. 5(c) and system voltages in Fig. 5(d) are discussed deeper in the above paragraph.

4.3 Case 3

The active power generated is depicted in Fig. 6(a). The reactive power generation of Fig. 6(b) for BT reminds of the results in Fig. 2(b). Synchronously operated 16 ⅔ Hz AC railway power systems are complex in their nature, and the exact reasons for this behaviour needs further investigations.

The CS currents are depicted in Fig. 7(a). Additionally, the rotor speed deviations are illustrated in Fig. 7(b), which are results in many ways reminding of the ones depicted in Fig. 3(b), but with the exception that the RFC in CS 2 oscillates more. That is natural since in Case 3, CS 2 contains an RFC of the Q38/Q39 type.

The train loads in Fig. 7(c) and the system voltages in Fig. 7(d) remind very much of the Case 1 results to be seen in Figs. 3(c) and 3(d).

4.4 Case 4

For both the AT and BT subcases of Case 4, the main difference between Figs. 8(a) and Fig. 4(a) of Case 2 is that CS 2 active power is smaller in Case 4 where CS 2 is smaller/ weaker than in Case 2. In regards of reactive power, depicted in Fig. 8(b), the BT results are very similar to the ones of Fig. 4(b) of Case 2, whereas the AT results of Case 4 show reduced levels of reactive power in the CSs in relation to Case 2. Last, but not least, during the fault, the reactive power output is severely reduced compared to the three other cases.

The currents of the CSs are shown in Fig. 9(a). The rotor speed deviations of Fig. 9(b) of Case 4 are in a sense similar to the ones of Fig. 5(b), with the exception that the equality in RFC populations of the two CSs makes all the speed deviations more synchronized. Train

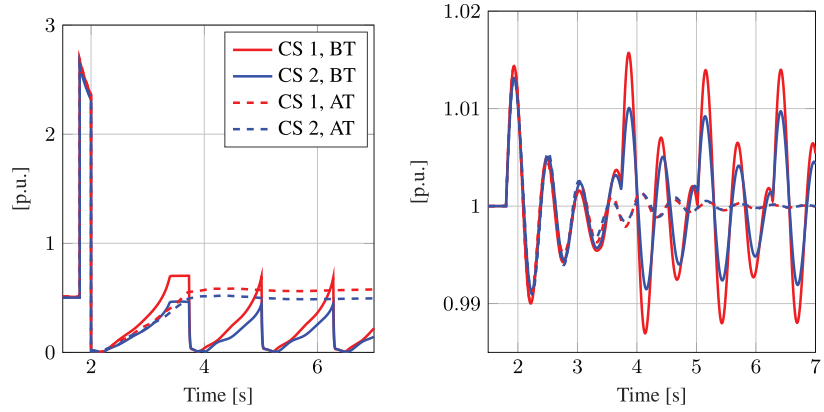

(a) The current levels of the converter(station)s in the system.

(b) The rotor speeds of the converter(station)s in the system. A useful legend is located in fig. 9(d).

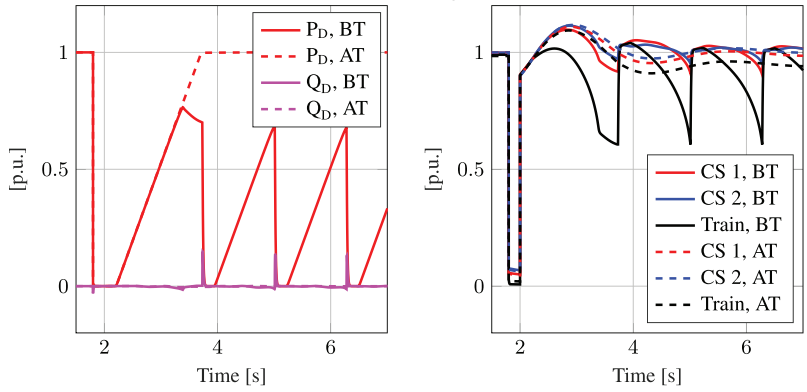

(c) The active and reactive power consumptions of the trains in the system.

(d) The voltage levels of the trains and the converter stations in the system.

Figure 9: Case 4, voltage regulated active power load.

loads and system voltages of Figs. 9(c) and 9(d) of Case 4 are very similar to the ones depicted in Figs. 5(c) and 5(d) of Case 2.

5 DISCUSSION AND CONCLUSIONS

The main intention with study was to increase the knowledge about transient stability of 16 ⅔ Hz synchronous railways. However, besides that, it also gave useful inputs for future studies about improved load sharing and voltage control for such power systems.

It is clearly illustrated that a synchronously operated, RFC-fed, low-frequency railway is transiently stable in the cases studied.

REFERENCES

[1] Laury, J., Abrahamsson, L. & Bollen, M., Transient stability of a rotary frequency converter fed railway, interconnected with a parallel low frequency high voltage transmission system. *WIT Transactions on the Built Environment*, **181**, 2018. https://doi.org/10.2495/cr180021

[2] Laury, J., Abrahamsson, L. & Bollen, M., Transient stability of rotary frequency converter fed low frequency railway grids: The impact of different grid impedances and different converter station configurations. *Proceedings of the ASME Joint Rail Conference*, Pittsburgh, PA: USA, 2018. JRC2018-6247

[3] Olofsson, M., *Investigations of transient stability in railway power supply (Original title in Swedish: Undersökning av transient stabilitet i matningssystem för elektrisk tågdrift)* [Master's Thesis]. KTH, Electric Power and Energy Systems, 1989.

[4] Laury, J., Abrahamsson, L. & Bollen, M.H.J., A rotary frequency converter model for electromechanical transient studies of 16⅔ Hz railway systems. *International Journal of Electrical Power & Energy Systems*, 106, pp. 467–476, 2019.

[5] Abrahamsson, L., *Railway Power Supply Models and Methods for Long-term Investment Analysis*. Technical report, Royal Institute of Technology (KTH), Stockholm, Sweden, 2008. [Licentiate Thesis].

[6] Olofsson, M., O*ptimal Operation of the Swedish Railway Electrical System - An Application of Optimal Power Flow* [Ph.D Thesis]. KTH, Stockholm, Sweden, 1996.

[7] Olofsson, M., *Power Flow Analysis of the Swedish Railway Electrical System*. Technical report, Royal Institute of Technology (KTH), Stockholm, Sweden, 1993. [Licentiate Thesis].

[8] Boullanger, B., *Modeling and Simulation of Future Railways* [Master's Thesis]. Royal Institute of Technology (KTH), 2009.

[9] Danielsen, S., *Electric Traction Power System Stability – Low-frequency Interaction Between Advanced Rail Vehicles and a Rotary Frequency Converter* [Ph.D. thesis]. NTNU, 2010.

[10] CENELEC – European Committee for Electrotechnical Standardization, Railway Applications – Power Supply and Rolling Stock. Technical Report EN 50388:2012, CENELEC–European Committee for Electrotechnical Standardization, 2012. [Standard].

[11] Abrahamsson, L. & Östlund, S., Optimizing the power flows in a railway power supply system fed by rotary converters. *Joint Rail Conference*, IEEE/ASME, 2015.

[12] Olofsson, M. & Thunberg, E., Optimal commitment of frequency converter units for railway power supply. *Railroad Conference*, 1999. *Proceedings of the 1999 ASME/IEEE Joint*, 1999.

[13] Abrahamsson, L., Jimenez, D.S., Laury, J. & Bollen, M., AC Cables Strengthening Railway Low Frequency AC Power Supply Systems. 2017 *Joint Rail Conferenc*e, Philadelphia, PA, USA, 2017. Paper No. JRC2017-2258